Acta Ciencia Indica, Vol. XLVII-M, No. 1 to 4, 17 (2021)

PERFORMANCE CHARACTERISTICS OF CELLULAR STRUCTURES FOR SOLAR ENERGY APPLICATIONS

PAWAN KUMAR SHARMA, KRITI GALAV AND CHANDRA SHEKHAR

Deptt of Maths, Bareilly College, Bareilly,

pksharma1170@gmail.com , kriti29596@gmail.com ,chandrashekharrithani@gmail.com

RECEIVED : 17 August, 2021

The paper presents design, development, fabrication and performance characteristics of cellular structures under the actual operating conditions for solar energy applications. Experimental results show that noryl air heater is capable of providing hot air of temperature difference [15^0 C-30^0 C] on a moderate sunny day. Therefore it is a suitable air heater for producing hot air of space heating and agricultural drying applications. Further computational results shows that cell width of 8-10 mm is required to suppress convection for the range of temperature difference as[50^0-100^0C] for 2 cm depth of honeycomb for providing the insulation in a solar pond. The computational results by Simpson's one-third rule for square celled honeycombs and parallel slat arrays shows that the ground diffuse radiation transmittance for Lexan honeycomb is maximum when the honeycomb is in vertical position while the sky diffuse radiation transmittance increases with increase in tilt angle and maximum in middle range and again decreasing with further tilt angle. The variation of transmittance in slats is also similar to the honeycomb. The transmittance shows decrease in trend with increase of aspect ratio. In the last the thermal performances of TIM application on the walls/roof of a building in Leh and Delhi have been investigated to maintain 20^0 temperature. The computational investigations for the effect of insulation on daily heat flux through walls/roof in a building at Leh region and Delhi region present the similar heating effect. The lower value of load leveling factor concludes the savings in air-conditioned heating load as well as cost.

Keywords: Insulation, TIM, Honeycomb, Slat device, Noryl air heater, solar pond, Transmittance.

INTRODUCTION

The cellular structure means a solar transparent device, which provide good thermal insulation by intercepting the incidental solar radiation and reduces its intensity. These

structures are generally known as transparent Insulation Materials devices (TIM), which may be classified as parallel-absorber, Vertical- Absorber, Cavity and Homogeneous structures based on their cellular geometry (Fig.1, Fig.2 and Fig.3). In vertical absorber structures cell walls are placed perpendicular to absorber plane. The major advantage ofthis configuration is forward reflection and re reflection of solar radiation by the vertical walls. Consequently, maximum amount of radiation reaches the absorber plane and hence vertical absorber structures are most suitable for development; it includes parallel slat arrays, honeycombs and capillaries.

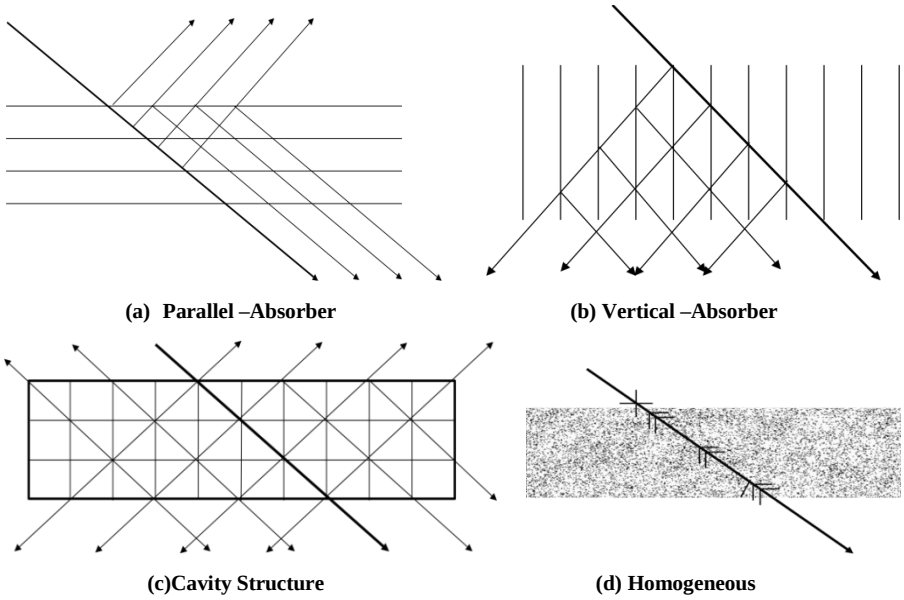

(a) Parallel –Absorber **(b) Vertical –Absorber**

(c)Cavity Structure **(d) Homogeneous**

Fig.1: TIM Structure

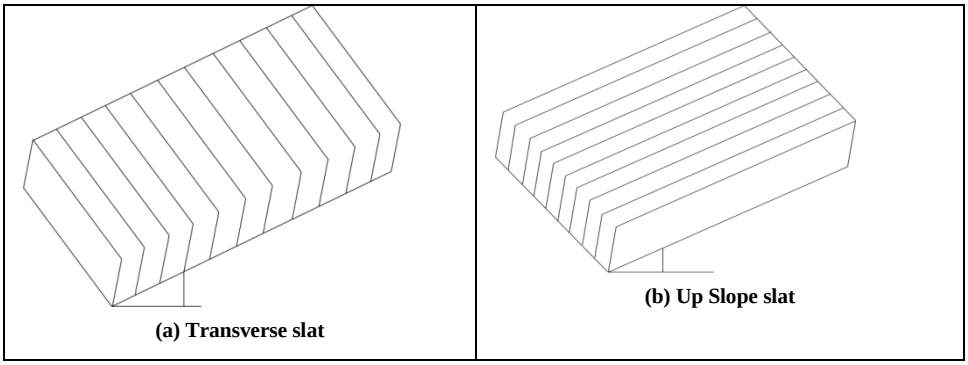

(a) Transverse slat **(b) Up Slope slat**

Fig. 2: Slat Structures

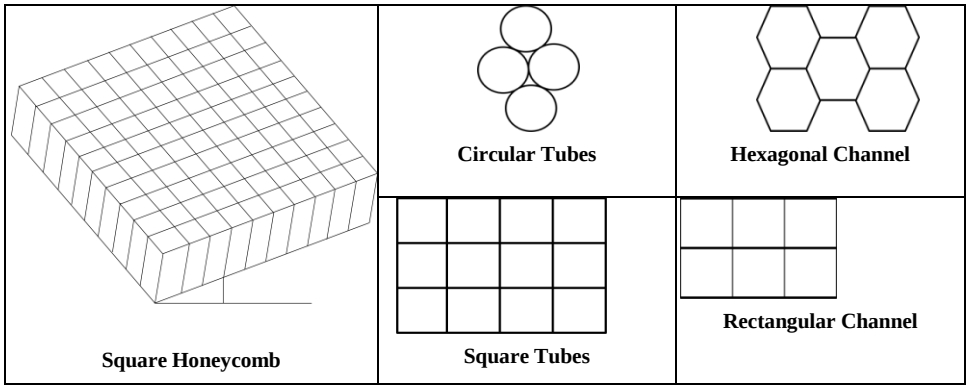

In these structures, Hexagonal shape of bee honeycomb can be economically used in two dimensional spaces. Further investigations have been made to design and fabricate the circular, square and rectangular cells. Fabrication methods of these devices have been represented in details in the final technical report of (CSIR- Research project no.23(156)/85/EMR-II) by Kaushika N.D.10 and Kaushika and Sumathy14. For the fabrication of most popular honeycomb modules of size (50 cm x 50 cm x 10 cm); the material is cut into slats of (50 cm □ 10 cm and then these slitted slats are interwoven to form a square cell array.

Proceeding in this way our intention goes to structured product (a range of Lexan polycarbonate sheets, profile, films and formed products) for a variety of application in buildings, construction signage and other industrial areas. we see that Lexan Multiwall sheet structures have an excellent energy saving insulation property. These sheets help us to save 50% of the energy costs in comparison to glass. These sheets can be represented by twin wall rectangular structure, Triple wall structure, Twin wall 'N' structure, Four wall rectangular structure and five wall rectangular structure (Fig. 4(A-E)) respectively:

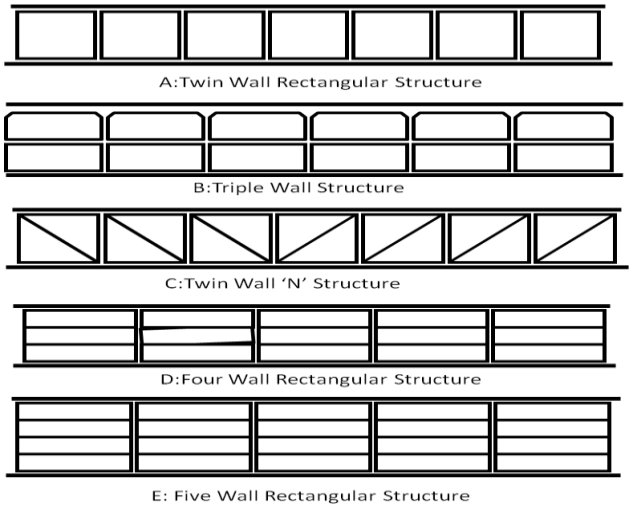

Fig. 4(A-E): Lexan Multiwall sheet structures

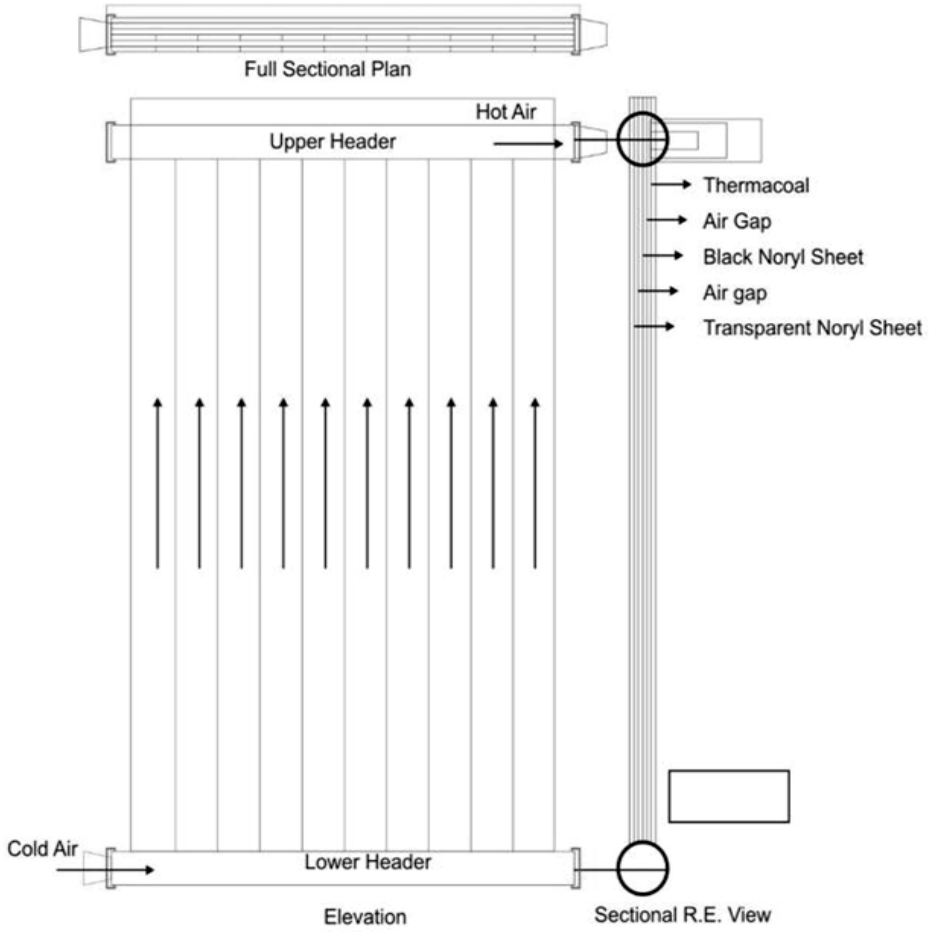

Continuing in this way we have design and fabricate the Noryl Air heater. This air heater consists of a plane black absorber sheet (1.25 m□ 1 m) made of noryl plastic material. The riser tubes are channel with a square cross section and are embodied in the absorber plate. The header tubes are PVCpipes of diameter 65 mm. The glazing is made of polycarbonate structured materials of thickness 10 mm. The airgap between the absorber and the glazing is 10 mm. The bottom insulation is provided by the thermocol sheet of 10 mm thickness. An air gap of 10 mm is provided between the black absorber and the bottom thermocol insulation. No way for thecollector box frame is provided instead the channels arecovered with wooden frame which provides the strength. Engineering drawing are given in Fig. 5.

In this experiment the diameter of inlet nozzle was 65 mm and that of outlet nozzle was 30 mm. Air velocity observed at the inlet was 0.2 m/s while atmospheric pressure was 750 mm of Hg. The collector was placed facing southward at an angle of 15^0 inclined to horizontal. The inlet and the outlet temperature have been measured with the help of nickel

and chromium thermocouples. Experimental results shows that noryl air heater is capable of providing hot air of temperature difference[15^0 C-30^0 C] on a moderate sunny day. Therefore it is a suitable air heater for producing hot air of space heating and agricultural drying applications.

Further in a observation we see that use of plastics has exhibited problem like loss of transmittance due to weather ability. Kaushika[9] has pave the way for development and wider application of honeycombs.

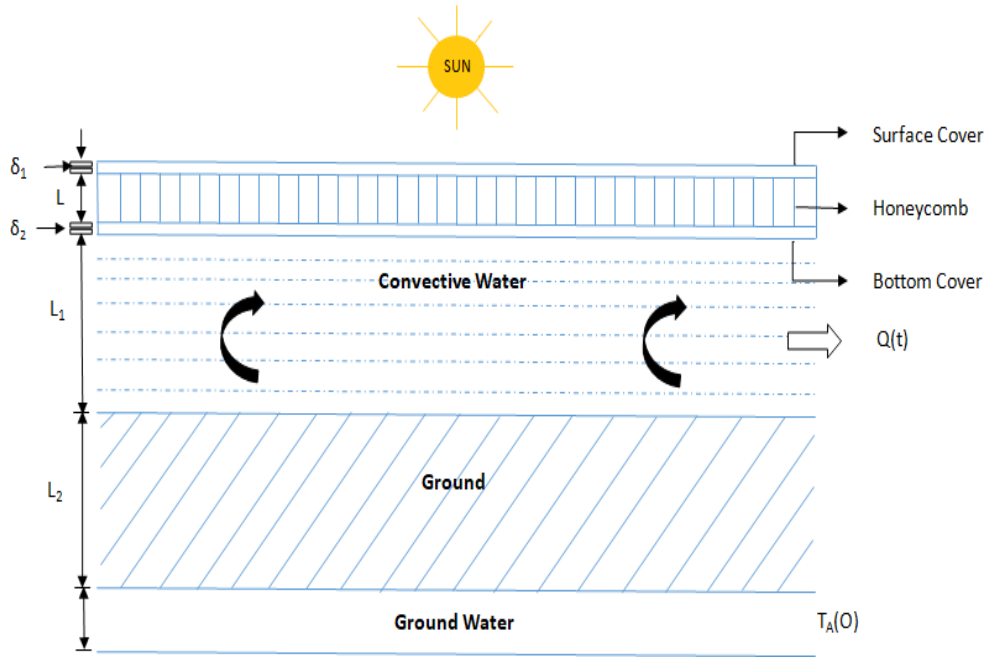

Continuing this process, an attempt has been made to design the honeycomb solar pond with a thin transparent cover at the surface and a thin transparent sheet or oil layer at its bottom represented by Fig.6. The performance characteristics of honeycomb solar pond for the square cells has been given by Lin[15], Ortabasi U.[17], Edwards and Catton[4], Sharma and Kaushika[8] etc. The solar pond proposed by Lin[15] is comprised of a sealed air filled honeycomb panel floating over a hot water reservoir that collects and concentrates solar thermal energy. The other configuration, proposed by Ortabasi et al.[17], consists of open honeycomb panels placed on a layer of oil floating on the body of warm water that collects solar thermal energy.

In above field experience we see that open honeycomb collects dirt etc. and loses its transmittance rapidly, while the transmittance of Lexan honeycomb is appreciable at all angles of incidence for solar pond applications, whereas the Transmittance of acrylic honeycomb is rather low and seems appropriate only for lower angle of incidence. Following above references for the performance characteristics of solar pond, R_c and R_a may be expressed as

$$R_c = \frac{({a_0}^2 + 23.9)^3}{({a_0}^2 + 7.97)} \; where \;\; a_0 = \; 0.75\pi A\sqrt{(5)} = 5.2686\, A \; and \; R_a = \frac{g\alpha \Delta T L^3}{k\nu} \quad \ldots (1)$$

So for convection suppression

$$(\Delta T)_{\max} = \frac{\mathrm{R_c k\nu}}{\mathrm{g\alpha L^3}} \quad \ldots (2)$$

For air we have

$$g = 9.8\frac{m}{s^2}, \kappa = 2.67 \times 10^{-5}\frac{m^2}{s}, \nu = 1.921 \times 10^{-5}\frac{m^2}{s},$$

$$\alpha = (2.97 \times 10^{-3})^0 c^{-1} \quad \ldots (3)$$

Therefore $$\frac{\kappa\nu}{g\alpha} = 17.622 \times 10^{-9} = \xi(say)$$

and $$(\Delta T)_{max} = \frac{\xi R_c}{L^3} \quad \ldots (4)$$

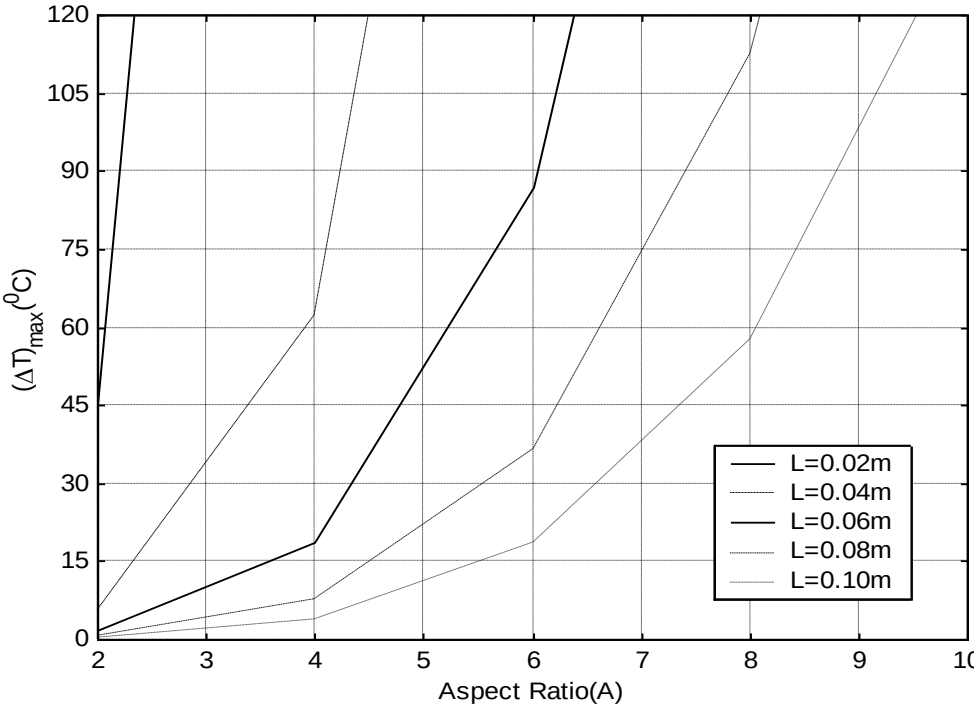

Where ξ is number, which has different values for different materials. The computed $(\Delta T)_{\max}$ values of air layer as obtained from equation (4) gives variation of $(\Delta T)_{\max}$ with aspect ratio (A) for honeycomb of depth L. We see that cell width of 8-10 mm is required to suppress convection for the range of temperature difference as [50^0-100^0C] for 2 cm depth of Honeycomb as shown in Fig. 7.

OPTIMISATION OF TIM PERFORMANCE

The solar collection effectiveness of a transparent cellular device can be judged by an accurate determinationof its solar transmittance. In practice the solar radiations is composed of beam and diffuse components and under certain situations the magnitude of diffuse components is significant. Solar beam radiation transmittance for these devices has been investigated by several authors e.g. Feland and Edwards[5] , Hollands et al.[7], Kaushika and Padmapriya[11], Platzer[6] , Kaushika N.D *et al*[13] ,Pawan Kumar Sharma *et al*[19] ; However diffuse radiation transmittance does not seem to have been investigated in detail, although it has been incorporated by Arulanantham and Kaushika[1]. The solar diffuse radiation consists of two components: sky diffuse and ground reflected one. The solar diffuse radiation transmittance of cellular arrays is investigated by integrating the beam transmittance over appropriate angle of incidence given by

$$\tau_d = \frac{\int_\omega \tau_b(\theta,\phi) I cos\theta d\omega}{\int_\omega I cos\theta d\omega}$$

where θ, ϕ and ω represents the angle of incidence , angle of azimuth and the angular angle of diffuse radiation respectively . The optical processes corresponding to incoming beam radiation has been represented by fig. 8.

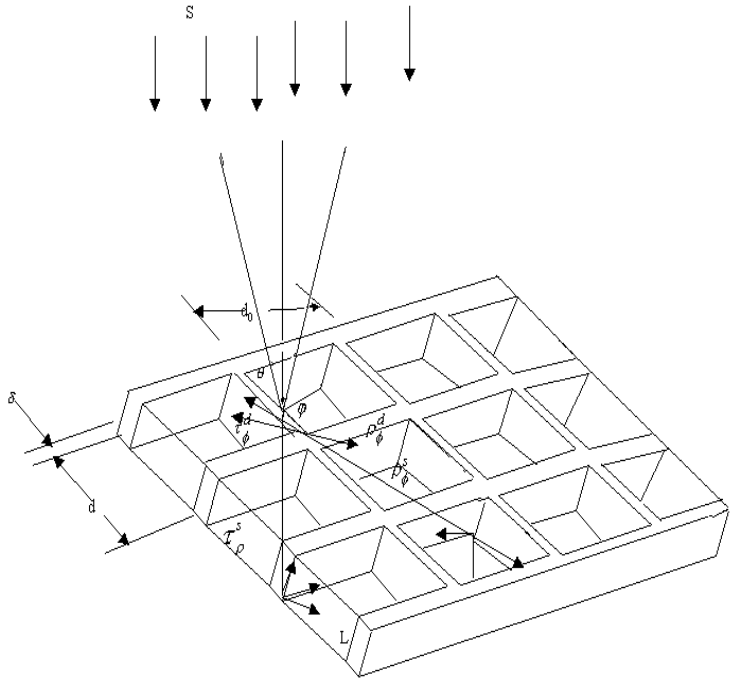

Fig.8: Optical process corresponding to incoming beam radiation

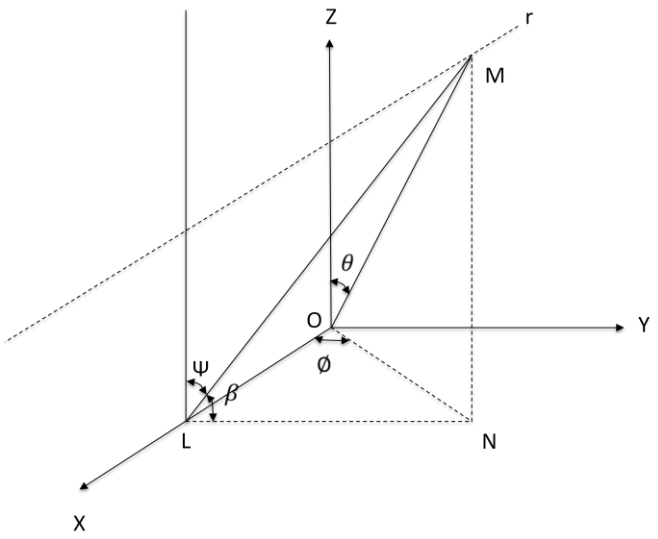

Fig.9: Spherical coordinate system for integration limits.

The solar beam radiation on the top of cellular matrix propagates through both cell and wall. The major portion propagating through the cells undergoes forward reflection towards absorber as well as refraction and absorption due to vertical walls. The radiation propagation through the walls is due to internal reflections. The beam radiation transmittance for honeycomb and slat Arrays τ_b (θ, ϕ) have been presented by Hollands et al.[7] and Arulanantham and Kaushika[1]. The diffuse radiation is assumed to be hemispherical in nature for which the solid angle d ω is given by $d\omega = \sin\theta d\phi d\theta$ .Therefore

$$\tau_d = \frac{\int_\omega \tau_b(\theta,\phi)\sin 2\theta \, d\phi d\theta}{\int_\omega \sin 2\theta d\phi d\theta} \quad \ldots (5)$$

Let us consider that Z axis is perpendicular to TIM (top surface) and x axis is parallel to ground. Consider that TIM is tilted at an angle β and the line r separates sky radiation from ground. For ground diffuse radiation transmittance θ varies from $\left(\frac{\pi}{2}-\beta\right)$ to $\frac{\pi}{2}$ and ϕ varies from $\sin^{-1}\left(\frac{\cot\beta}{\tan\theta}\right)$ to $\pi-\sin^{-1}\left(\frac{\cot\beta}{\tan\theta}\right)$ represented by Brandemuehl and Beckman[2] as shown in Fig. 9. The line r is parallel to x- axis at a unit distance from x axis and at an angle Ψ from XZ plane. From Fig. 9, we have $\psi=\left(\frac{\pi}{2}-\beta\right)$, which $\tan\psi=\left(\frac{\pi}{2}-\beta\right)=\cot\beta=\frac{LN}{MN}$, $\sin\phi=\frac{LN}{ON}$ and $\tan\theta=\frac{ON}{MN}$, Therefore

$$\tan\psi=\frac{LN}{MN}=\left(\frac{LN}{ON}\right)\times\left(\frac{ON}{MN}\right)=\sin\phi\tan\theta$$

and hence $$\phi = \sin^{-1}(\cot\beta / tan\,\theta) \quad \ldots (6)$$

Using these integration limits and axial symmetry, the ground diffuse radiation transmittance, τ_{dg} is given by

$$\tau_{dg} = \frac{\int_{\frac{\pi}{2}-\beta}^{\frac{\pi}{2}} \int_{\sin^{-1}\left(\frac{\cot\beta}{\tan\theta}\right)}^{\frac{\pi}{2}} \tau_b(\theta,\phi)\sin 2\theta\, d\phi\, d\theta}{\int_{\frac{\pi}{2}-\beta}^{\frac{\pi}{2}} \int_{\sin^{-1}\left(\frac{\cot\beta}{\tan\theta}\right)}^{\frac{\pi}{2}} \sin 2\theta\, d\phi\, d\theta} \quad \ldots(7)$$

For sky diffuse radiation transmittance θ varies from 0 to $\frac{\pi}{2}$ and for incidence angle $\theta \le \frac{\pi}{2} - \beta$ the angle ϕ will vary from 0 to 2π. For $\theta \ge \frac{\pi}{2} - \beta$, ϕ varies from $\phi = \pi - \sin^{-1}\frac{\cot\beta}{\tan\theta}$ to $\phi = 2\pi + \sin^{-1}\frac{\cot\beta}{\tan\theta}$. Applying these integration limits and the axial symmetry we get the sky diffuse radiation transmittance given by

$$\tau_{ds} = \frac{\int_0^{\frac{\pi}{2}-\beta} \int_{-\frac{\pi}{2}}^{\frac{\pi}{2}} \tau_b(\theta,\phi)\sin 2\theta\, d\phi\, d\theta + \int_{\frac{\pi}{2}-\beta}^{\frac{\pi}{2}} \int_{\frac{-\pi}{2}}^{\sin^{-1}\left(\frac{\cot\beta}{\tan\theta}\right)} \tau_b(\theta,\phi)\sin 2\theta\, d\phi\; d\theta}{\int_0^{\frac{\pi}{2}-\beta} \int_{-\frac{\pi}{2}}^{\frac{\pi}{2}} \sin 2\theta\, d\phi\, d\theta + \int_{\frac{\pi}{2}-\beta}^{\frac{\pi}{2}} \int_{-\frac{\pi}{2}}^{\sin^{-1}\left(\frac{\cot\beta}{\tan\theta}\right)} \sin 2\theta\, d\phi\, d\theta} \quad \ldots (8)$$

The overall diffuse radiation transmittance for the insulation device is given by

$$\tau_{do} = \frac{\tau_{ds} + \rho\,\tau_{dg}}{1+\rho} \quad \ldots (9)$$

where ρ is the ground reflectance

Numerical computation of integral equation (7) and (8) for ground and sky diffuse radiation transmittance of square celled honeycombs and parallel slat arrays are carried out by Simpson's one-third rule. The optical parameters used in computation are summarized in Table1.

Table 1

Parameter	ρ_{ve}^{s}	ρ_{ve}^{d}	A	M	Depth
Acrylic	0.95	0.013	0.037	1.49	1 mm

Glass	0.94	0.015	0.045	1.5	1mm
Polycarbonate	0.977	0.023	0.0001	1.54	0.076 mm

The computational results for the ground and sky diffuse radiation transmittance for Lexan honeycomb of 10 cm thickness are shown by Fig. 10 & Fig. 11 respectively. Fig. 10 shows that the ground diffuse radiation transmittance is maximum when the honeycomb is in vertical position. From Fig.11, we conclude that the sky diffuse radiation transmittance for Lexan honeycomb increases with increase in tilt angle and maximum in middle range and again decreasing with further tilt angle.

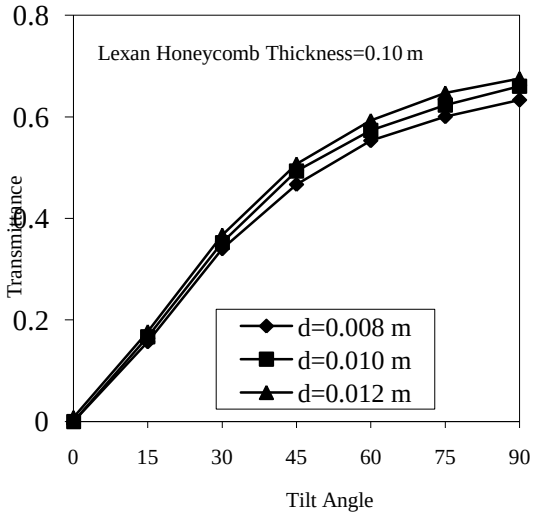

Fig.10:Ground Diffuse Radiation Transmittance for Lexan Honeycomb

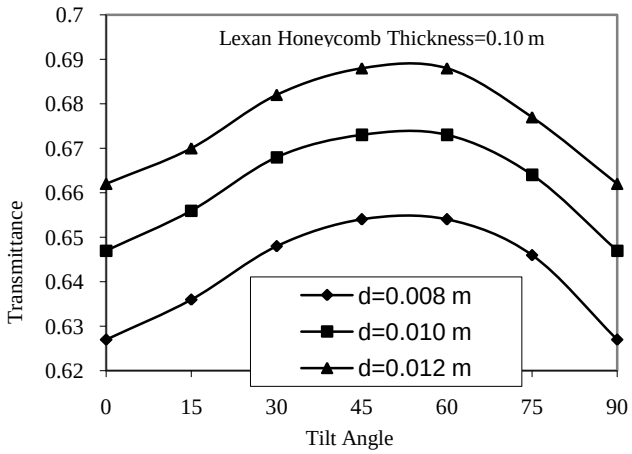

Fig.11. Sky diffuse radiation transmittance for Lexan honeycomb.

The ground and sky diffuse radiation transmittance for Lexan slat of thickness 5 cm are shown by Fig. 12 & Fig.13 respectively. The variation of transmittance in slats is similar to the honeycomb. In all the four Fig.(10,11,12,13,) the transmittance shows decrease in trend with increase of aspect ratio. The variation of transmittance in slats is similar to the honeycomb.

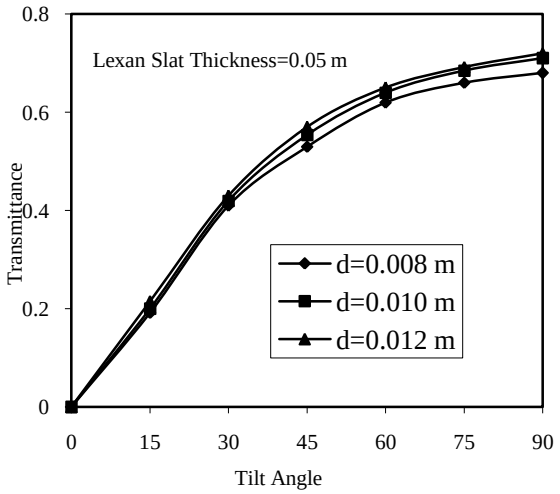

Fig.12: Ground Diffuse Radiation Transmittance for Lexan slats

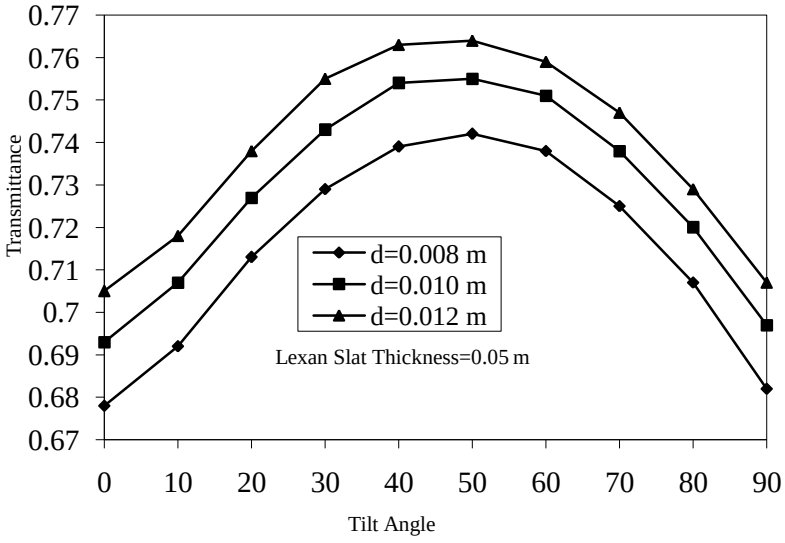

Fig.13: Sky Diffuse Radiation Transmittance for Lexan Slats

Thermal performance of TIM applications in a building

In thermal performance evaluation of TIM application on the walls/roof of a building; The metrological data for Leh (Latitude =34^0 09'N, Longitude =77^{0}34' E, Altitude=3414m) and Delhi(Latitude=28^0 35'N, Longitude=77^{0}12' E, Altitude=216m) have been taken from hand book of solar radiation by Mani[16] and Bansal N.K. et. al[3]. The formula used for solar irradiance on wall and roof of the building for the tilted surface is

$$I_t(t) = I_{hb}(t)\, R_b(t) + I_{hd}(t)\, R_d(t) + I_{hg}(t)\, R_r \qquad ...(10)$$

where $R_b(t) = \dfrac{\cos\theta_i}{\cos\theta_z}$, $R_d(t) = \dfrac{1+\cos\beta}{2}$, $R_r = \dfrac{\rho(1-\cos\beta)}{2}$,

$$\cos\theta_z = \cos\phi\cos\delta\cos\omega + \sin\delta\sin\phi$$

The angle of incidence θ_i $(0 \le \theta_i \le 90)$ vary with hour angle ω as :

For $\cos\omega > \dfrac{\tan\delta}{\tan\phi}$;

$$\cos\theta_i = \cos\delta\cos\omega\sin\phi\cos\gamma\sin\beta - \sin\delta\cos\phi\cos\gamma\sin\beta + \cos\delta\ \sin\omega\ \sin\gamma\sin\beta + \cos\beta\cos\phi\cos\delta\cos\omega + \cos\beta\sin\phi\sin\delta \qquad ...(11)$$

and for $\cos\omega < \dfrac{\tan\delta}{\tan\phi}$;

$$\cos\theta_i = -\cos\delta\cos\omega\sin\phi\cos\gamma\sin\beta + \sin\delta\cos\phi\cos\gamma\sin\beta + \cos\delta\ \sin\omega\ \sin\gamma\sin\beta + \cos\beta\cos\phi\cos\delta\cos\omega + \cos\beta\sin\phi\sin\delta \qquad ...(12)$$

Heat transfer through bare roof /walls is given by

$$Q(t) = U(T_{SA} - T_R) \qquad ... (13)$$

Where U is the over all heat transfer through bare roof/wall given by

$$U = \frac{1}{\frac{1}{h_0} + \frac{L}{K} + \frac{1}{h_i}} \qquad ... (14)$$

T_{SA} is the solair temperature given by

$$T_{SA} = \frac{\alpha\ I_t(t) - \varepsilon\Delta R}{h_0} + T_A \qquad ...(15)$$

T_A is the ambient temperature, T_R is the room temperature, α is absorptivity,h_0 is the loss coefficient made up of convective h_c and radiative h_r component *i.e.* $h_0 = h_c + h_r$. The resultant heat flux through bare (walls and roof) is given by

$$Q_b(t) = Q_{bst} + Q_{bn\,t} + Q_{bet} + Q_{bwt} \qquad ...(16)$$

The resultant heat flux per day through bare (walls and roof) is given as

$$Q_{bwr} = \sum_{t=1}^{24} Q_b(t) \text{ Kwh} \quad ...(17)$$

T_{SA} for insulated wall/roof is given by

$$T_{SA} = \frac{(\alpha\tau)_{eff} \; I_t(t) - \varepsilon \Delta R}{U_L} + T_A \quad ...(18)$$

Over all heat transfer through insulated wall/roof is given as:

$$U_t = \frac{1}{\frac{1}{h_t} + \sum \frac{L}{K} + \frac{1}{h_i}} \quad ...(19)$$

And heat transfer through insulated wall/roof is given as

$$Q(t) = U_t (T_{SA} - T_R) \quad ... (20)$$

Thus the resultant heat flux$Q_i(t)$ through insulated south wall and others bare wall/roof is

$$Q_i(t) = Qst + Qnt + Qet + Qwt + Qrt \quad ... (21)$$

So the resultant heat flux per day through insulated south wall and bare (walls and roof) is given as

$$Q_{iwr} = \sum_{t=1}^{24} Q(t) \text{ Kwh} \quad ...(22)$$

The heat transfer coefficient and other thermophysical parameters used in this computation are listed below:

α =0.9, h_0 = 22.7796 W/m^2 ^{0}C, h_i = 6.817212 W/m^2 ^{0}C, h_t = 2.1 W/m^2 ^{0}C, L = thickness of concrete wall/roof=0.10 m K=Thermal conductivity of concrete wall/roof = 0.72228W/m K, $\varepsilon \Delta R = 0$ for bare walls and $\varepsilon \Delta R = 61.1 W/m^2 K$ for bare roof & $\varepsilon \Delta R = 0.0 W/m^2 K$ for insulated wall/ roof.

The computational results for solar radiation intensity on walls/roof for Leh and Delhi region show that the Solar radiation intensity is very small on North wall and it increases on west wall from morning to evening. Simultaneously The solar radiation intensity first increases and then decreases on east wall from morning to evening, while we get maximum intensity on south wall and then on roof. So we plan to insulate South wall first and then roof by lexan honeycomb on it for heating purpose of the building to maintain 20^0 temperature. The computations have been carried out using the MATLAB software. The computational results for resultant hourly heat flux through bare roof& walls with and without insulation on south wall in w/m^2 in Leh and Delhi region are shown in Fig. 14 & Fig.15 respectively.

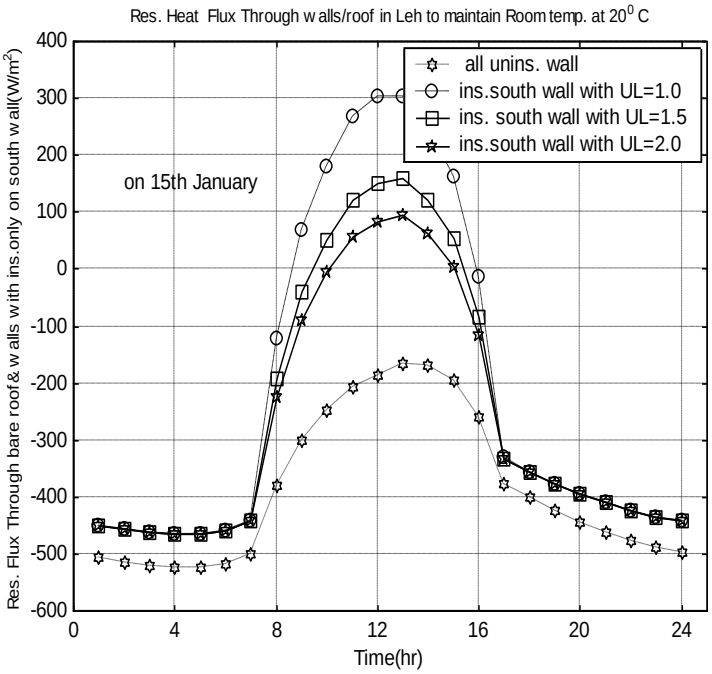
Res. Heat Flux Through walls/roof in Leh to maintain Room temp. at 20^0 C
all unins. wall
ins.south wall with UL=1.0
ins. south wall with UL=1.5
ins.south wall with UL=2.0
on 15th January
Res. Flux Through bare roof& walls with ins.only on south wall(W/m^2)
Time(hr)

Fig. 14

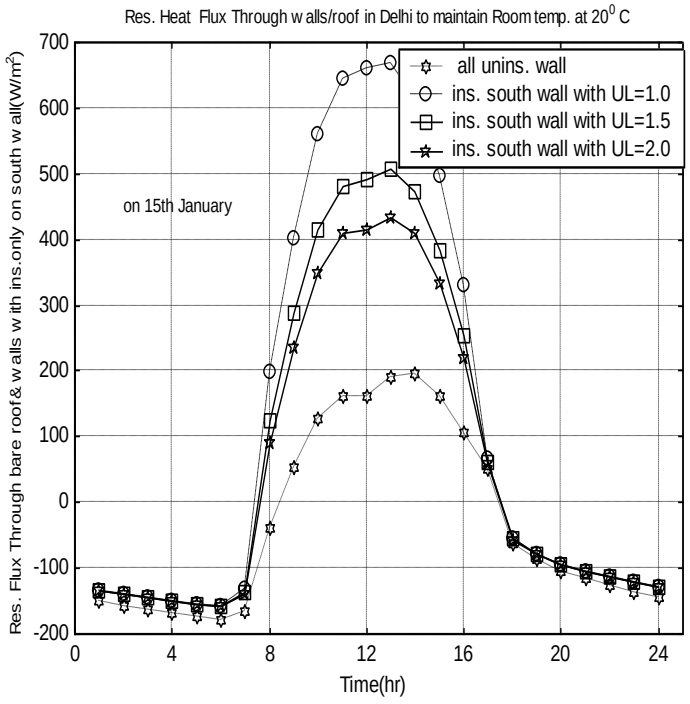
Res. Heat Flux Through walls/roof in Delhi to maintain Room temp. at 20^0 C
all unins. wall
ins. south wall with UL=1.0
ins. south wall with UL=1.5
ins. south wall with UL=2.0
on 15th January
Res. Flux Through bare roof& walls with ins.only on south wall(W/m^2)
Time(hr)

Fig. 15

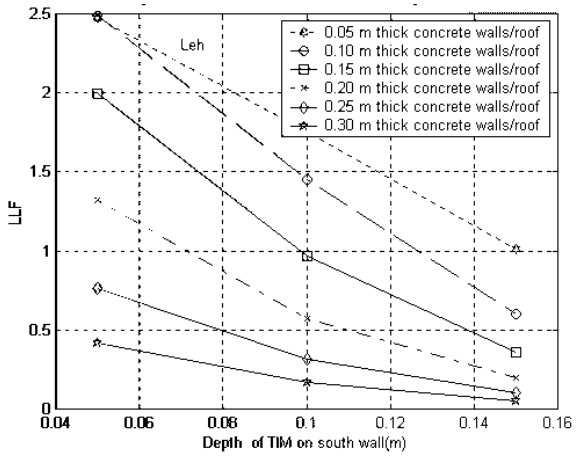

Fig. 16

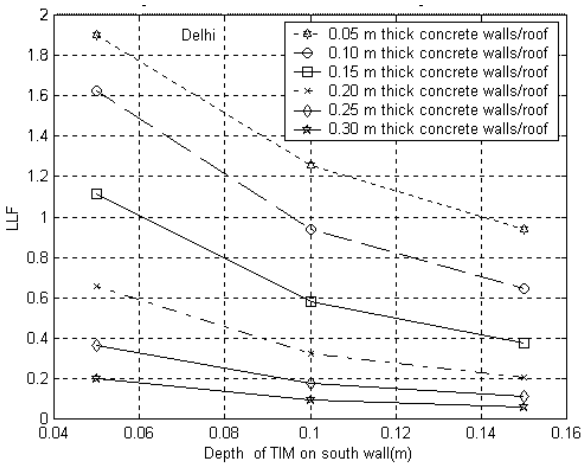

Fig. 17

It is seen that placement of TIM insulation device on south wall enhances the heat flux and hence reduces the air conditioning heating load. A panel of depth 0.10m-0.15m seems suitable for significant energy conservation in buildings of cold climates. The capacity and the capital cost of an air-conditioning plant is determined by the range of thermal load. We have, therefore examined the load levelling of heat flux entering the indoor space in Fig. 16 and Fig. 17. The simulation results indicate significant reduction of load levelling factor with thickness of TIM cover as well as concrete walls/roof thickness. Larger thickness of TIM cover and the walls/roof would obviously involve higher costs. The lower values of load leveling factor corresponds to savings in air-conditioned heating load as well as cost. The reduction in load leveling factor would also correspond to reduction of control strategies to prevent overheating and discomfort in the living space.

The auther wish to acknowledge the help and discussion with Prof. N.D. Kaushika of the Centre for EnergyStudies, IIT New Delhi.

REFERENCES

1. M, Matsumoto: On Riemannian spaces with recurrent projective curvature, *Tensor (N.S.)*, **19**, 11-17, (1968).
2. Arulanantham M. and Kaushika N.D.. Global Radiation Transmittance of Transparent Insulation Materials. *Solar Energy*, **53** (4) : 323-328 (1994).
3. Brandemuehl, M. J. and Beckman, W.A.. Transmission of Diffuse radiation through CPC andflat plate collectors glazing. *Solar Energy*, **24**, 511 (1980).
4. N.K Bansal, S.N.Garg, N. Lugani and M. S. Bhandari, Determination of glazing area in direct gain systems for three different climatic zones, *Solar Energy* **53**(1), 81-90 (1994).
5. Edwards, D.K. and Catton, I. Prediction of heat transfer by natural convection in closed cylindersheated from below. Int. J. Heat and Mass Transfer 12-23 (1969).
6. Feland, J. R. and Edward, D.K.. Solar and Infrared radiation properties of parallel platehoneycomb. J. of Energy, **2**, 275 (1978).
7. Platzer W.J., Solar Transmission of transparent Isulation Materials. *Solar Energy Materials*, **16**, 275 (1987).
8. Hollands K. G. T., Marshall K. N. and Wedel R.K. An approximate equation for predicting the solar transmittance of transparent honeycombs, **Solar energy**, **21**, 231 (1978).
9. Sharma, M.S. and Kaushika N.D. Design and performance characteristics of honeycomb solarpond. *Energy convers. Mgmt.*, **32**, 345 (1987).
10. Kaushika N.D. Solar Ponds: A Review, Energy convers. Mgmt. **23**,1 (1984).
11. Kaushika, N.D., Design and Development of honeycomb and slat convection suppression devices for solar energy applications. Final Technical Report of CSIR Research project No. **23** (156)/ 85/EMR-II (1989).
12. Kaushika, N.D. and padmapriya, R. Solar transmittance of honeycomb and Parallel slat arrays. *Energy convers. Mgmt.*, **32**, 345 (1991).
13. Kaushika N.D., Sharma P.K. and Padmapriya R,. Solar thermal analysis of honeycomb roof cover system for energy conservation in an air conditioned building, *Energy and Building*, 18, 45 (1992).
14. Kaushika N.D.,Priya padma, Arulanantham M. and Sharma P.K.. Transparent insulation Characteristics of Honeycomb and Slat arrays. Energy Volume **19**, No. 10. pp. 1037-1041 (1994).
15. Kaushika N.D and Sumaty K,. Solar transparent insulation materials:A review, *RenewableSustainable Energy Rev*, N0 7, pp 317-351 (2003).
16. Lin E.I.H., Progr. *Solar Energy(Am. Section of Int Solar Energy Soc.*) p.215 (1982).
17. Mani,Anna, 1980. Hand Book of Solar Radiation data for India. New Delhi, Allied Publishers,
18. Ortabasi U., Dyksterhuis F.M. and Kaushika N.D.,1983, Honeycomb Stabilized Saltless Solar Pond,Solar Energy 31,229-231.
19. Pawan Kumar and Kaushika N.D., 2005. Convective effects in air layer bound by cellular honeycomb arrays. Journal of Scientific and Industrial Research, Vol **64**, pp 602-612.
20. Pawan Kumar Sharma, Kriti Galav and Chandra Shekhar. Transparent Insulation Materials Devices For Sustainable Development and Energy Audit in Buildings. International Journal of Creative Research Thoughts (IJCRT), Volume 8, 772-793 (2020).
21. Smart D R, Hollands KGT& Raithby G D. . free convection heat transfer across rectangular celled diathermous honeycomb,Trans ASME J Heat Mass Transfer,102, pp 75-80 (1980).

❑